

The Use of Ultrasound for the Electrochemical Precipitation of Struvite

Faranak Foroughi^a, Md. H. Islam^a, Jacob J. Lamb^a???, László Kékedy-Nagy^b, Lauren F. Greenlee^b and Bruno G. Pollet^{a*}

^a Hydrogen Energy and Sonochemistry Research group, Department of Energy and Process Engineering, Norwegian University of Science and Technology (NTNU), Trondheim 7491, Norway

^b Ralph E. Martin Department of Chemical Engineering, University of Arkansas, 3202 Bell Engineering Center, Fayetteville, AR 72701, USA

With the observed global intensification of the agricultural sector, slurry management has now become a severe problem. This has resulted in a large amount of pollution from agriculture, mainly due to the excessive use of industrial fertilizers and pesticides. This pollution results in the increase of microorganisms and the leaching of pollutants into the surrounding environment. Therefore, it is imperative that these waste slurries are not stored for long periods of time and treated on-site. Furthermore, the efficient extraction of biologically useful nutrients (e.g., nitrogen, phosphorus) will allow the production of renewable fertilizers. This present work highlights the recovery of these nutrients by electrochemical precipitation of struvite in the presence of ultrasound using magnesium (Mg) electrodes. It was observed that the combination of electrochemistry and ultrasound can facilitate and accelerate the production of struvite.

Introduction

The presence of harmful bacteria, viruses and other micro-organisms induced by poor manure management is causing pollutants to enter the surrounding environment (e.g., soil, water and air contamination). Consequently, the sector has set some urgent priorities. An example priority is to minimize storage and encourage the treatment of wastewater and solid slurries by reducing energy consumption, and by creating on-site renewable energy systems (ref). This could be possible by coupling the waste streams to anaerobic digestion (1). Furthermore, most of the agricultural manures contain useful nutrients such as nitrogen (N), phosphorus (P) and potassium (K), and efficiently extracting them to produce added-value products, could significantly reduce the environmental impacts and reduce the requirement of commercial fertilizers. Therefore, it is important to implement novel, efficient and clean environmental and energy technologies with the view of recycling important nutrients from agricultural sludges and wastes.

Struvite (magnesium ammonium phosphate—MAP: $MgNH_4PO_4 \cdot 6H_2O$) crystallization is an efficient method to recover useful nutrients such as P and N from wastewater (2, 3), urine (4, 5) and manure (6, 7). Struvite is considered as a slow release fertilizer that can be used for agriculture if the properties of the final product can be controlled (8). Struvite usually forms as orthorhombic crystals according to equation [1], where n = 0, 1 or 2 based on the solution pH (9).



The formation process consists of two chemical stages: nucleation and crystal growth (10). Controlling of these stages is governed by the thermodynamics of the solid-liquid equilibrium, the mass transfer between solid/liquid phase (10) and the reaction kinetics (9). Struvite crystallization is also managed by the combination of the primary concentration of the ionic species in solution, the pH, the speed of mixing and the presence of foreign ions (9).

There are different processes to recover struvite such as chemical (11), biological (12) and physical (13). In this work we introduce sonoelectrochemical precipitation of struvite on Mg electrode plates, an application where the use of ultrasound is in combination with electrochemistry. Ultrasound refers to an acoustic wave with a frequency above 20 kHz, whereas an input of power equal to 10 W or above is known as the ultrasonication range (14). These waves can be directly or indirectly transmitted through a transducer and into a medium. Acoustic cavitation and streaming are the major effects induced by propagation of an acoustic wave into the medium. Cavitation itself results in small gas bubbles forming that oscillate as a consequence of the acoustic wave. These gas bubbles eventually collapse and generate temperatures of up to 5000°C and pressures up to 2000 atmosphere (15). The collapse causes the transmission of both chemical/ mechanical effects into the medium and results in the formation of a variety of radicals and reactive species from water through sonolysis (i.e., HO·, O₃, H₂O₂ and O) (16). These species diffuse into the medium and may react with nearby solutes and has been recently observed to improve degradation of rigid and obstinate biochemical compounds (17).

Sonoelectrochemistry was first introduced in water electrolysis using platinum (Pt) electrodes in the 1930s by the work of Moriguchi et al (16). Ultrasound irradiation in electrochemistry offers many advantages including: disruption of the diffusion layer, degassing at the electrode surface or the solution, cleaning and activation of the electrode surface, and improvement of the mass transport of ions across the double layer

(14, 16, 18).

Acoustic streaming, turbulent flow, microjets and shock waves are the major influencing factors of ultrasound in electrochemistry (16). The main effects of acoustic streaming is the enhancement of the solution movement, reducing the diffusion boundary layer and increasing the mass transfer of electroactive species to the electrode surface (16). Turbulent flow is caused by the movement of the acoustic cavitation bubbles (16). It enhances the mass transport process within the solution and the electrode surface similar to acoustic streaming. The collapsing of acoustic bubbles on a solid surface leads to the formation of microjets being directed towards the surface of the solid material at speeds of up to 200 m/s (19). Microstreaming is caused by the bubbles close to the surface. If the surface is an electrode, the combined effects of the microjet and microstreaming increase mass transport to the electrode surface (14).

Induction of ultrasound to the crystallization solution affects the crystallization process by enabling modifications and improvements of the process and physical properties of the product (20). Ultrasound has a high impact on effective mixing (21) and for preparing homogeneous suspensions. In addition, ultrasound avoids the agglomeration of the obtained product. In general, sonication of the reaction mixture causes radiation microstreaming (21), and high local temperature and pressure (22), also known as the driving forces for mass transfer (21) and cavitation (21). Consequently, the energy and mass transfer is faster, reducing the thermal and concentration gradient, thus increasing the formation of the product (23). High pressure and temperature is originated from the cavitation bubbles within the medium and acts as seeds or foreign particles in the suspension, which facilitates heterogeneous crystallization in the fastest way at a defined

point (21). As a result, the use of ultrasound in the crystallization process promotes diffusion and reduces the nucleation time and the free critical energy (21).

To the best of our knowledge, sonoelectrochemical precipitation of struvite has not been reported. In the present study, we used ultrasound power for electrochemical precipitation of struvite and compared our results with the electrochemical precipitation of struvite without ultrasound. It was observed that ultrasound has an effective influence on the crystallization of struvite. In addition, the effect of ultrasound on the electrochemical behavior of the platinum electrode in a dihydrogen ammonium phosphate electrolyte has been investigated.

Experimental

Materials

The experiments were performed at room temperature with aqueous solutions containing 0.3 M of ammonium dihydrogen phosphate ($\text{NH}_4\text{H}_2\text{PO}_4$) from Sigma-Aldrich. The solutions were prepared by using ultrapure water (14.46 MΩ.cm, StakPure GmbH, Germany). The magnesium foil (99.9% pure), the AZ31 magnesium alloy foil (Al 3 wt%, Zn 1 wt%, balance Mg) and the stainless-steel (316SS) were all purchased from Goodfellow. The plates were mechanically polished with different grain size (240, 800, 1200) abrasive papers (Norton Abrasives), followed by 5 and 0.3 μm alumina suspension (Allied high tech products). The pH of the bulk test solution was determined before and after the experiments by using a digital pH meter (Memosens, KNIK).

Reactor setup and open circuit potential (OCP) measurements

The OCP measurements were conducted in a sonoelectrochemical reactor filled with approx. 500 mL of the solution which was sonicated by ultrasonic bath (VWR, 45 kHz 300 W, Malaysia). A refrigerated circulator (JULABO, Germany) was connected to the reactor in order to keep the reactor at the room temperature. Thin plates of Pure Mg/an AZ31 Mg and 316SS with active surface area of ($\sim 40 \text{ cm}^2$), were used as anode and cathode, respectively. The OCP of the system was carried out with a potentiostat/Galvanostat/ZRA (Gamry instruments, USA) and it was referred against an Ag/AgCl (3M KCl) electrode. OCP experiments without ultrasound were carried out in an 800 mL beaker in which the solutions were stirred continuously by a magnetic stirrer (IKA RCT-classic).

Electrochemical behavior of the platinum electrode in ammonium dihydrogen phosphate with and without ultrasound

Electrochemical behavior of platinum electrode in ammonium dihydrogen phosphate aqueous solution with and without ultrasound was studied by cyclic voltammetry. A Gamry potentiostat/galvanostat was used for the electrochemical measurements with a three-electrode cell system consisting of Ag/AgCl (3 M KCl) as the reference- and a platinum (Pt) wire as the auxiliary electrode, respectively. A Pt disk? (Metrohm, Germany??, diameter 1 mm) served as the working electrode. The measurements were carried out in Nitrogen-saturated ammonium dihydrogen phosphate aqueous solution (0.3 M) at a scan rate of 50 mV s^{-1} . Before measurements the platinum electrode was cleaned with 0.3 and 0.05 μm alumina and sonicated for 10 min in ethanol. The ultrasound frequencies of 45 kHz and 24 kHz were vibrated to platinum electrode by ultrasonic bath (VWR, Malaysia) and ultrasonic processor (Heilscher, UP400St, 400 W), respectively.

Characterization of the precipitates

Scanning electron microscope (LVSEM, Hitachi S-3400 N) was used to study the effect of ultrasound on the morphology of the produced precipitate (struvite).

Result and Discussion

OCP measurements in the presence and absence of ultrasound

Figure 1 shows the OCP plots of pure Mg and AZ31 alloys in presence and absence of power ultrasound, respectively. As can be seen in Figure 1, an abrupt change in the OCP towards the positive potentials in the presence of ultrasound for both anodes is significantly higher than the OCPs recorded in silent condition. This suggests that the formation (nucleation) of struvite layer on the anodes in presence of ultrasound was faster. This is because the use of ultrasound can trigger crystallization through saturation conditions. Moreover, the heterogeneous crystallization was facilitated by cavitation bubbles that acted as foreign particles (seeds) in the solution (23).

The OCP plots for both anodes in the presence and absence of ultrasound didn't become steady within 6 hours suggesting that the corrosion of anodes continued but the rate of corrosion with ultrasound was higher. This behavior is associated with the activation and cleaning of the electrode by ultrasound that doesn't allow the formation of a compact layer on the electrode surface to prevent further corrosion. Electrode cleaning and surface activation is due to the microjets that result from the collapsing of acoustic bubbles. This prevents fouling of the electrode surface and the accumulation of gas bubbles at the electrode surface, and increases the electrodeposition process (14).

The pure Mg plate in presence of ultrasound shows a sudden decrease in potential after approximately 3 hours, which then started to increase again (Figure 1a, blue line). This can be also related to the implosion of acoustic cavitation bubbles at the electrode surface that clean the surface and create new nucleation sites (14, 20). Once the newly active sites of surface filled up the OCP started to increase again towards positive potentials.

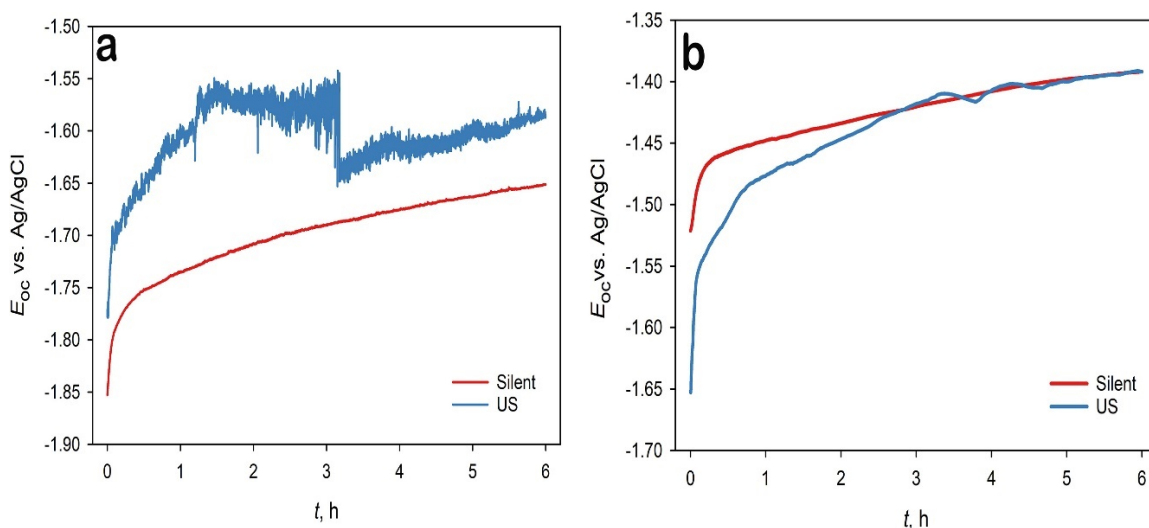


Figure 1. The OCP measurements of a) pure-Mg, and b) AZ31 alloy as anodes in 0.3 M ammonium dihydrogen phosphate aqueous solution with and without ultrasound.

Gravimetric analysis was performed to evaluate the estimated corrosion losses of the pure Mg and AZ31 alloy. As observed in Figure 2, the pure Mg plates showed a greater weight loss with and without ultrasound than AZ31 alloy. In addition, the plates that were treated by ultrasound illustrated more corrosion loss. The higher weight loss suggested a higher corrosion rate, which in turn produced a higher struvite amount.

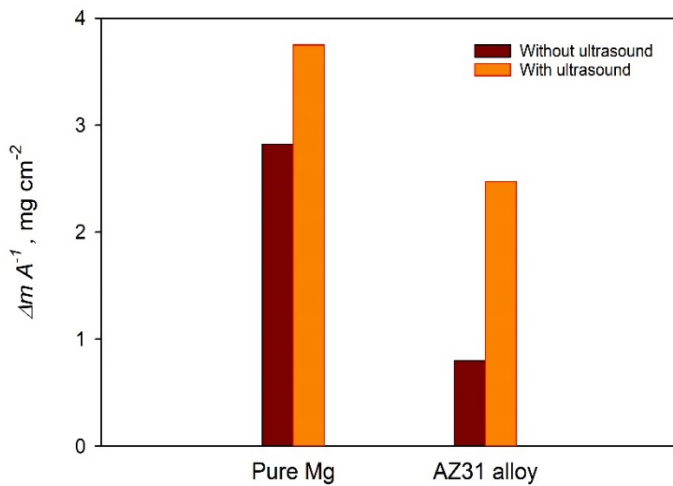


Figure 2. The weight losses of Pure Mg and AZ31 alloy after 6 hours of OCP measurements.

Figure 3 illustrates the pH differences in the bulk solution measured before and after the OCP measurements with and without ultrasound. As can be observed, ultrasound causes higher change in the solution pH. The pH is usually used as an indicator of struvite nucleation (9), where the change in the pH occurs during the nucleation process. The increase in the pH is characteristic of the rate at which the first crystals of struvite occurs, and is linked to the speed of formation of struvite (9). Therefore, ultrasound could cause an increase in the pH and a reduction in the induction time, subsequently enhancement of struvite formation.

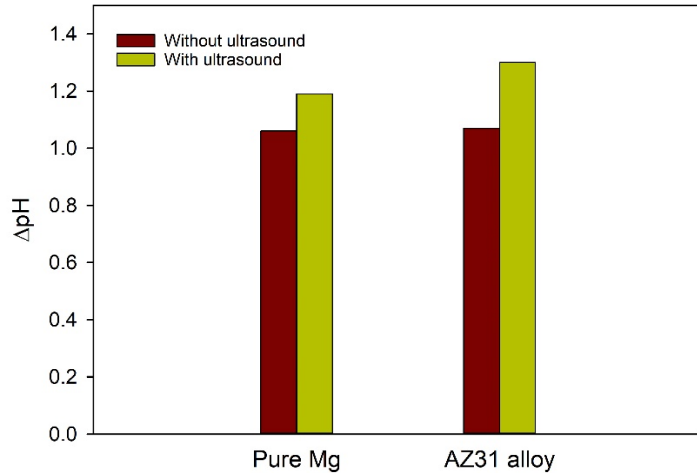


Figure 3. The pH difference in the bulk solution after 6 hours OCP measurements.

Characterization of the precipitate

Product particle size requirements largely depend on the final application. For example, a larger size is favored when struvite is used as a fertilizer, as it is easier to handle, transport, and apply. However, an increase in size also leads to a slower fertilizer release rate, due to a lower surface area/volume ratio (24). The influence of ultrasound power on the struvite crystal properties, were studied by scanning electron microscope (SEM). Figure 4 and 5 show the SEM images obtained of struvite layers on pure Mg and AZ31Mg in the absence and presence of ultrasound, respectively. As can be seen in both Figure 4b and 5b, the ultrasound-assisted crystallization leads to non-agglomerated struvite crystals. As it was previously mentioned, ultrasound significantly improves the mixing efficiency resulting in a homogeneous suspension and the avoidance of agglomeration (20). In addition, the high quality of the obtained products remained. The heterogeneous crystallization was facilitated by cavitation bubbles that acted like foreign particles (seeds) in the medium (20). Figure 4a and 5a illustrate compact layer forms on pure Mg and AZ31 alloy plates without ultrasound. This uniform and compact layer has a negative effect on struvite production that prevents further corrosion of the plates. This behavior could be attributed to more increase in the pH in the presence of ultrasound, which caused an increase of supersaturation and the growth rate (25).

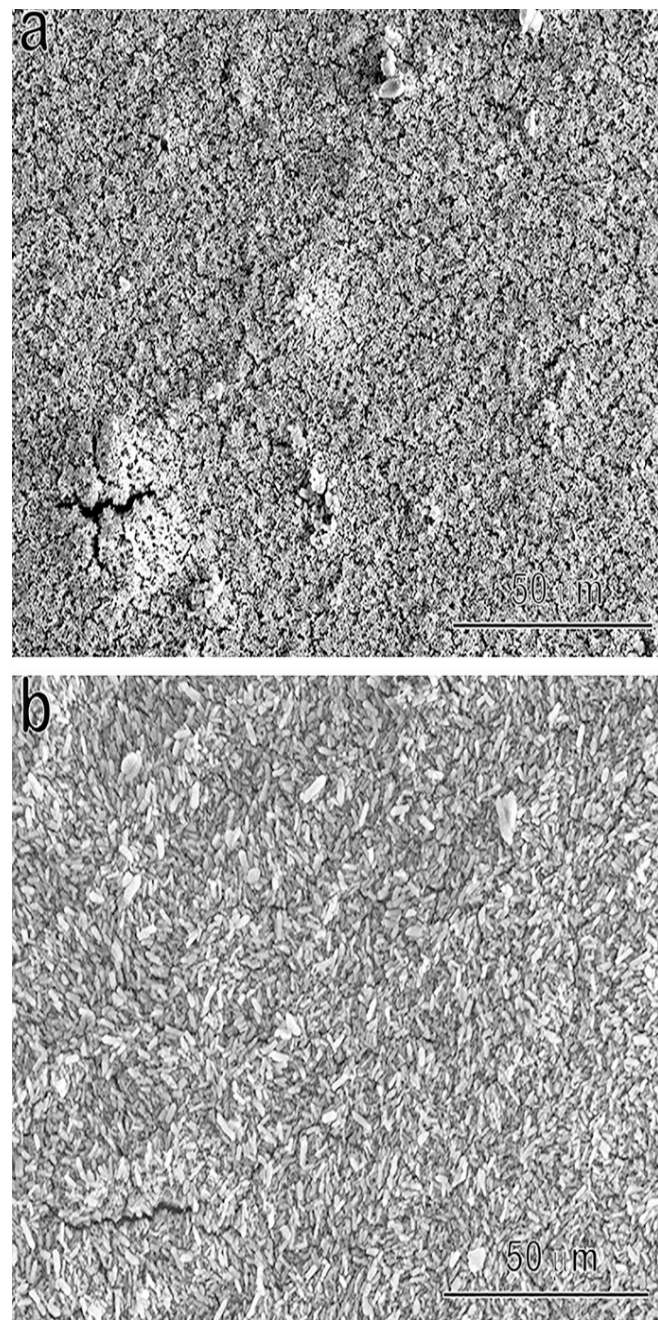


Figure 4. The SEM images obtained for struvite on pure Mg anodes a) without ultrasound, and b) with ultrasound.

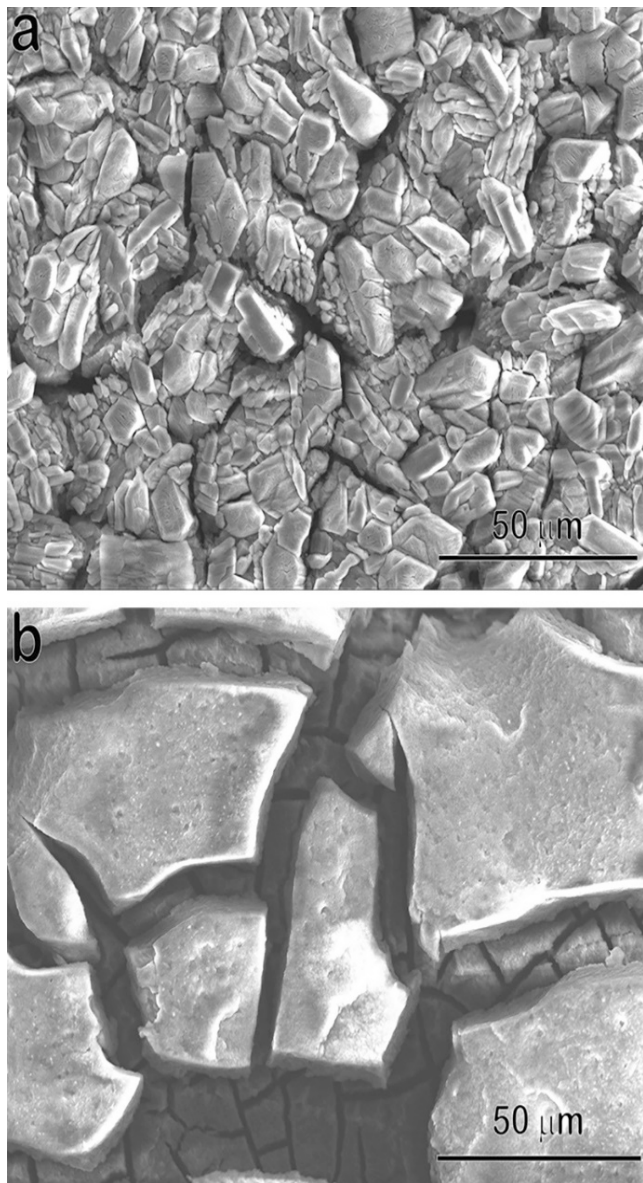


Figure 5. The SEM images obtained for struvite on AZ31 alloy anodes a) without ultrasound, and b) with ultrasound.

Electrochemical behavior of the platinum electrode in ammonium dihydrogen phosphate with and without ultrasound

The electrochemical response of the Pt electrode in 0.3 M ammonium dihydrogen phosphate (pH \sim 4.25) in the presence and absence of ultrasound was investigated. As can be seen in Figure 6, the characteristic shape of the cyclic voltammograms (CVs) of the platinum electrode in ammonium dihydrogen phosphate with and without ultrasound are similar to CVs in X M sulfuric acid. It can be observed that ultrasound would shift the oxidation/reduction Pt peaks to a more negative potential, and as the frequency of ultrasound increase the current of oxidation and reduction peaks decrease. According to Figure 6, the peaks and shoulders between -0.2 V and -0.4 V are attributed to the hydrogen adsorption/desorption region. At lower ultrasound frequencies, the intensity of peaks and shoulders of hydrogen desorption/adsorption are greater because of the increase in proton reduction due to enhanced diffusion. Contrary to this, the peaks of hydrogen desorption

and adsorption would be diminished at higher ultrasound frequencies, possibly due to the strong stirring of the solution (26) and consequently limitation of the proton diffusion (26).

The electrochemically active surface area (ECSA) was determined from the charge due to the desorption of hydrogen measured from CVs recorded at 50 mV/s between -0.2 V and -0.4 V vs. Ag/AgCl in N₂-purged ammonium dihydrogen phosphate aqueous solution. According to this, ECSAs of 1.78, 1.93 and 0.0042 mm² were obtained for platinum with no ultrasound, 24 kHz ultrasound and 45 kHz ultrasound conditions, respectively. The low ECSA of the higher ultrasound frequency could be related to a smaller hydrogen desorption peak and subsequently less Q_H. As discussed above, a high frequency would decrease the reduction of protons.

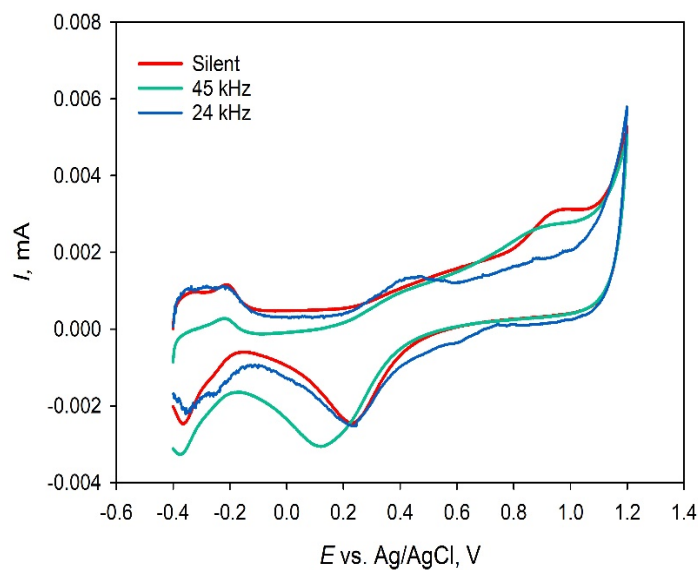


Figure 6. The cyclic voltammograms of Pt electrode obtained with and without ultrasound in 0.3 M ammonium dihydrogen phosphate aqueous solution at the scan rate of 50 mV s⁻¹.

Conclusion

In this research, the effect of ultrasound on the electrochemical production of struvite by using pure Mg and AZ31 Mg alloy as anode was investigated. The results indicate that by the ultrasound-assisted crystallization, struvite was successfully produced faster in comparison to the conventional electrochemical method. Since the cavitation bubbles behave as foreign particles, deagglomeration was eliminated. Furthermore, the induction of ultrasound to the solution increased the mass of the product, which is caused by activation and cleaning of surface. These results suggest that ultrasound-assisted production of struvite could be a potential route for extraction of nutrients from agricultural and bioenergy wastes, allowing their utilization as fertilizers for terrestrial food crops.

Acknowledgments

The authors would like to acknowledge the support from the ENERSENSE research initiative at NTNU.

References

1. S. Sarker, J. J. Lamb, D. R. Hjelme and K. M. Lien, *Applied Sciences*, **9**, 1915 (2019).
2. K. Suzuki, Y. Tanaka, K. Kuroda, D. Hanajima and Y. Fukumoto, *Bioresource technology*, **96**, 1544 (2005).
3. S. Lee, S. Weon, C. Lee and B. Koopman, *Chemosphere*, **51**, 265 (2003).
4. M. Ronteltap, M. Maurer and W. Gujer, *Water Research*, **41**, 977 (2007).
5. J. Wilsenach, C. Schuurbiers and M. Van Loosdrecht, *Water research*, **41**, 458 (2007).
6. I. Çelen, J. R. Buchanan, R. T. Burns, R. B. Robinson and D. R. Raman, *Water Research*, **41**, 1689 (2007).
7. R. Schuiling and A. Andrade, *Environmental Technology*, **20**, 765 (1999).
8. N. Booker, A. Priestley and I. Fraser, *Environmental Technology*, **20**, 777 (1999).
9. K. S. Le Corre, E. Valsami-Jones, P. Hobbs and S. A. Parsons, *Journal of crystal growth*, **283**, 514 (2005).
10. A. G. Jones, *Crystallization process systems*, Elsevier (2002).
11. Z. Li, X. Ren, J. Zuo, Y. Liu, E. Duan, J. Yang, P. Chen and Y. Wang, *Molecules*, **17**, 2126 (2012).
12. F. Simoes, P. Vale, T. Stephenson and A. Soares, *Scientific reports*, **8**, 7225 (2018).
13. S. Regy, D. Mangin, J. P. Klein, J. Lieto and C. Thornton, *Laboratoire d'Automatique et de Génie des Procédés (LAGEP)*, 1 (2002).
14. M. H. Islam, O. S. Burheim and B. G. Pollet, *Ultrasonics sonochemistry* (2018).
15. K. S. Suslick, *science*, **247**, 1439 (1990).
16. J. Hihn, F. Touyeras, M. Doche, C. Costa and B. Pollet, Power Ultrasound in Electrochemistry: From Versatile Laboratory Tool to Engineering Solution, in, J. Wiley & Sons, Chichester (2012).
17. J. J. Lamb, M. H. Islam, D. R. Hjelme, B. G. Pollet and K. M. Lien, *Ultrasonics Sonochemistry*, 104675 (2019).
18. B. G. Pollet, *Ultrasonics sonochemistry*, **52**, 6 (2019).
19. S. A. Elder, *The Journal of the Acoustical Society of America*, **31**, 54 (1959).
20. L. M. Belca, A. Ručigaj, D. Teslić and M. Krajnc, *Ultrasonics Sonochemistry*, 104642 (2019).
21. K. Wohlgemuth, A. Kordylla, F. Ruether and G. Schembecker, *Chemical Engineering Science*, **64**, 4155 (2009).
22. T. J. Mason, *Progress in biophysics and molecular biology*, **93**, 166 (2007).
23. Z. Guo, A. Jones and N. Li, *Chemical Engineering Science*, **61**, 1617 (2006).
24. M. M. Rahman, M. A. M. Salleh, U. Rashid, A. Ahsan, M. M. Hossain and C. S. Ra, *Arabian journal of chemistry*, **7**, 139 (2014).
25. K. S. Le Corre, E. Valsami-Jones, P. Hobbs and S. A. Parsons, *Critical Reviews in Environmental Science and Technology*, **39**, 433 (2009).
26. C. Le Naour, P. Moisy, J. Léger, C. Petrier and C. Madic, *Journal of Electroanalytical Chemistry*, **501**, 215 (2001).